ELSEVIER

Spectrochimica Acta Part A 53 (1997) 1527–1536

SPECTROCHIMICA ACTA PART A

Time resolved study of CN band emission from plasma generated by laser irradiation of graphite

S.S. Harilal, Riju C. Issac, C.V. Bindhu, Pramod Gopinath, V.P.N. Nampoori, C.P.G. Vallabhan *

Laser Division, International School of Photonics, Cochin University of Science and Technology, Cochin 682 022, India

Received 16 December 1996; accepted 8 March 1997

Abstract

Time and space resolved studies of emission from CN molecules have been carried out in the plasma produced from graphite target by 1.06 μm pulses from a Q-switched Nd:YAG laser. Depending on the laser pulse energy, time of observation and position of the sampled volume of the plasma, the features of the emission spectrum are found to change drastically. The vibrational temperature and population distribution in the different vibrational levels have been studied as functions of distance, time, laser energy and ambient gas pressure. Evidence for nonlinear effects of the plasma medium such as self focusing which exhibits threshold-like behaviour are also obtained. Temperature and electron density of the plasma have been evaluated using the relative line intensities of successive ionization stages of carbon atom. These electron density measurements are verified by using Stark broadening method. © 1997 Elsevier Science B.V.

Keywords: Laser ablation; Graphite plasma; CN bands; Emission spectroscopy

1. Introduction

In the last few years there has been an ever growing interest in the investigations concerning the composition and evolution of the laser produced plasma from graphite [1–5]. One of the increasingly utilized plasma technologies for thin film preparation is pulsed laser deposition, in which a laser is focused onto a solid target and the resulting vapour plume is collected onto the substrate of interest [6–8]. Pulsed laser ablation of high purity graphite is considered to be one of the effective methods for deposition of diamond-like carbon (DLC) thin films [9–15]. Large area films of optical quality and uniformity have been grown in vacuum [9,10] and in gas mixtures containing hydrogen by several workers [16,17]. The physical properties of the plasma plume such as temperature and species concentration directly affect the properties of such thin films. Many of the laser ablation experiments were performed in order to understand the chemical reactivity of the neutral and charged particles produced in the plasma under the action of laser beams. It has been verified that the high proportions of ions to neutrals in the plasma produced by laser ablation

* Corresponding author. E-mail: root@cochin.ernet.in

PII S1386-1425(97)00062-0

are mainly responsible for uniform quality of the diamond-like carbon films [18].

Laser ablation is also a convenient method for producing highly stable carbon clusters such as C_{60} and higher fullerene molecules [19,20]. The presence of different species such as atomic, ionic and molecular carbon in the plume was found to depend on laser intensity [21]. The nature and characteristics of the laser induced plasma (LIP) from a solid target depend on various parameters such as chemical composition of the target, wavelength of irradiation, energy deposited on the target, ambient gas pressure inside the plasma chamber etc. [22–25]. It has been observed that the quality of the film is affected by the energy of the particle being deposited and hence, depends on the temperature. Therefore to optimize the film characterization it is necessary to estimate the temperature of the emitted species.

The pulsed radiation from a high power laser usually generates intense plasma emission from the target. A variety of techniques can be employed for characterizing laser induced plasma (LIP). Different types of plasma diagnostics techniques have been extensively reviewed [6,26]. Of these, time of flight mass spectroscopy [27,28], optical emission spectroscopy [29,30], optical absorption spectroscopy [31], line broadening [32], laser induced fluorescence [33] Langmuir probe method [34] and interferometry [35] are especially popular. Optical spectroscopy is an effective as well as convenient tool to detect various transient species such as excited atoms, ions and diatomic/polyatomic molecules, all of which are produced during laser ablation. Photography and other imaging techniques add another dimension to plasma diagnostics [36,37].

Depending on the time of observation and position of the sampled volume the features of the plasma emission change as the plasma expands. In the case of LIP from graphite target, the emission contains molecular band systems from different species such as C_2, CN etc. It has been pointed out that the excited diatomic species, which are sources of band emission in the different regions of plasma, may be formed by a secondary photolysis of the initial products. The CN violet system ($B^2\Sigma^+ \rightarrow X^2\Sigma^+$) has been studied by a variety of techniques [38–40] since it is an important free radical occurring in many emission sources. Even though a few studies are available in the literature related to CN species in the plasma, a systematic investigation of spatial and temporal variations of the characteristics of the plasma have not been reported yet. In this paper we describe in detail the spatial, temporal, laser energy and ambient gas pressure dependence of the CN species generated in graphite plasma by 1.06 μm pulsed laser irradiation under partial vacuum. The vibrational temperature and its variations under different conditions have been evaluated from the emission spectrum of CN violet band.

2. Experimental

Schematic diagram of the experimental technique is shown in Fig. 1. Plasma was generated by laser ablation of the high purity graphite sample using 1.06 μm radiation pulses from a Q-switched Nd:YAG laser [Qunata Ray DCR 11] having pulse width 9 ns and repetition rate 10 Hz. The estimated laser spot size at the target was 200 μm. The target in the form of a disc (25 mm diameter and 5 mm thickness) was placed in a partially evacuated chamber provided with optical windows for laser irradiation and spectroscopic observation of the plasma produced from the target. The target was rotated about an axis parallel to

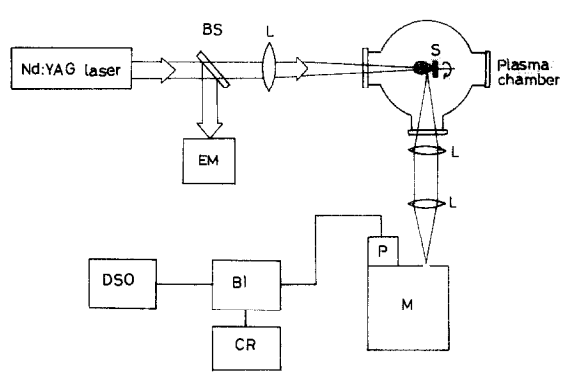

Fig. 1. Schematic diagram of the experimental set up. BS, beam splitter; EM, energy meter; L, lens; S, sample; M, monochromator; P, PMT; BI, boxcar averager/gated integrator; CR, chart recorder; DSO, digital storage oscilloscope.

the laser beam to avoid nonuniform pitting of the target surface. The bright plasma emission was viewed through a side window at right angles to the plasma expansion direction. The line of sight intensity of the plasma is collected from a cross section of area 0.01 cm^2. The section of the plasma was imaged onto the slit of a 1 m monochromator (Spex model 1704 with entrance and exit slits parallel to the target surface having widths 20 μm each, grating with 1200 grooves mm^{-1} blazed at 500 nm, maximum resolution 0.005 nm) using appropriate collimating and focusing lenses so as to have one to one correspondence with the sampled area of the plasma and the image. The scan of the monochromator was controlled using Spex CD2A compudrive arrangement. The recording was done by using a thermoelectrically cooled Thorn EMI Photo Multiplier Tube (PMT) (KQB 9863, rise time 2 ns, quantum efficiency 22%), which was coupled to a boxcar averager/gated integrator [Stanford Research Systems SR 250]. For spatially resolved studies different regions of the plasma plume were focused on to the monochromator slit. In our case the accuracy in spatial settings was better than 0.2 mm. The averaged output from the boxcar averager was fed to a chart recorder, which for the present study averaged the intensities from 10 pulses.

3. Results and discussion

3.1. Emission spectra

The spectra of the LIP from graphite target were recorded in the region $\lambda\lambda$ 350–600 nm. The emission spectra were intensity-normalized using the optical response curves of the monochromator—PMT assembly. All the emission intensities are corrected for the detector spectral response which is predetermined through use of a standard lamp. The emission spectrum is found to contain different vibrational bands of CN molecules in addition to atomic and ionized species of carbon. The intensities of the band emission has been found to depend on the delay time and distance from the target surface. Near the target surface atomic as well as ionic species predominate while in regions away from the target molecular species such as CN and C_2 dominate. The atomic, ionic and molecular carbon ejected from the target due to laser ablation combines with the ambient nitrogen present inside the plasma chamber resulting in the formation of CN molecules. Characteristic spectral emission of CN molecule in the violet region is obtained from the $B^2\Sigma^+ \rightarrow X^2\Sigma^+$ transition [41]. Well defined bands in sequences $\Delta v = 1, 0, -1, -2$ are recorded, where $\Delta v = v' - v''$ is the difference between the vibrational quantum numbers of the upper ($B^2\Sigma^+$) and lower ($X^2\Sigma^+$) electronic states.

3.2. Electron temperature and electron density measurements

3.2.1. Stark broadening method

The number density of electrons in a plasma can be obtained from the Stark broadened line profile of an isolated atom or singly charged ion with reasonable accuracy. In order to estimate the electron density we utilized the Stark broadened profile of C II transition at 392 nm ($3p^2p^0 - 4s^2S$) keeping the monochromator at its maximum resolution. The full width at half maximum (FWHM) of the line $\Delta\lambda_{1/2}$ is related to the electron density N_e by the expression [42,43]

$$\Delta\lambda_{1/2} = 2W\left[\frac{N_e}{10^{16}}\right] + 3.5A\left[\frac{N_e}{10^{16}}\right]^{1/4}\left[1 - \frac{3}{4}N_D^{1/3}\right]W\left[\frac{N_e}{10^{16}}\right]A^0 \quad (1)$$

where W is the electron impact parameter which can be incorporated to different temperatures [42]; A, ion broadening parameter and N_D, the number of particles in the Debye sphere. The first term in the right side of Eq. (1) represents the broadening due to electron contribution and the second term is the ion correction factor. For nonhydrogenic ions Stark broadening is predominantly by electron impact. Since the perturbations caused by ions are negligible compared with electrons, the ion correction factor can safely be neglected. Therefore Eq. (1) reduces to

$$\Delta\lambda_{1/2} = 2W\left[\frac{N_e}{10^{16}}\right]A^0 \quad (2)$$

The time integrated electron density is 1.58×10^{17} cm^{-3} at a distance 3 mm from the target and at a laser power density 4.95×10^{10} W cm^{-2}.

3.2.2. Relative line intensity measurements

The electron temperature and electron density of the LIP can be evaluated from the emission spectra of the ablated plume. For these calculations of N_e and T_e, the relative intensities of the same emitting species at successive stages of ionization were utilized. At LTE we have the relation [42]

$$\frac{I'}{I} = \left[\frac{f'g'\lambda^3}{fg\lambda'^3}\right][4\pi^{3/2}a_0^3N_e]^{-1}\left[\frac{kT_e}{E_H}\right]^{3/2} \times \exp\left[-\frac{E' + E_\infty - E - \Delta E_\infty}{kT}\right] \quad (3)$$

where the primed symbols represent the line of the atom with higher ionization stage; f, is the oscillator strength; g, statistical weight; a_0, Bohr radius; E_H, ionization energy of the hydrogen atom; E, excitation energy and ΔE_∞ is the reduction in the ionization energy E_∞ of the lower ionization stage. The correction factor in the ionization energy is given by [42]

$$\Delta E_\infty = 3z\frac{e^2}{4\pi\epsilon_0}\left[\frac{4\pi N_e}{3}\right]^{1/3} \quad (4)$$

where $z = 2$ for the lower ionization state. The correction factor in the ionization energy is found to be 0.008 eV at $N_e = 10^{17}$ cm^{-3}.

For the evaluation of T_e and N_e, we make use of registered line intensities from the lines at 464.7 and 569.6 nm of C III and 392 and 407.4 nm lines of C II. The calculated values of T_e and N_e at a distance 3 mm from the target and at a laser irradiance of 4.95×10^{10} W cm^{-2} are 2.05 eV and 1.23×10^{17} cm^{-3} respectively. The small variation occurred in the calculation of Ne using Stark broadening and line intensity measurements can be attributed to the uncertainty in the values of oscillator strengths and the electron impact parameter.

The calculations of T_e and N_e were carried out from Stark broadening and line intensity measurements under the assumption that the plasma is in LTE. It is clear that LTE will be approached only at sufficiently large particle densities. A necessary (but not sufficient) criterion for LTE is that [43]

$$N_e \geq 1.4 \times 10^{14}T_e^{1/2}(\Delta E_{mn})^3 \text{ cm}^{-3} \quad (5)$$

where T_e is in eV, ΔE_{mn} is the energy difference between upper and lower energy levels (in eV). For the transition at 392 nm, $\Delta E_{mn} = 3.16$ eV, the lowest limit for N_e is 6.3×10^{15} cm^{-3}. Our calculated values of N_e are much greater than this limit implying that LTE approximation for these analysis are valid.

3.3. Vibrational temperature analysis of CN molecules

The electronic transition of diatomic molecules often possess band structures due to the many vibrational levels. Molecules in a certain vibrational state v' of the upper electronic state can decay to different vibrational levels v'' of the lower electronic state giving subsequently the emission intensities $I(v', v'')$. According to the vibrational sum rule for intensities of different bands in a progression, the sums of the band strengths of all bands with the same upper or lower states are proportional to the number of molecules in the respective states [44], i.e.

$$\sum_{v''}\frac{I(v', v'')}{\upsilon^4} \propto N_{v'} \quad (6)$$

$$\sum_{v'}\frac{I(v', v'')}{\upsilon^4} \propto N_{v''} \quad (7)$$

where υ is the frequency in cm^{-1}, $N_{v'}$, and $N_{v''}$, the numbers of the molecules in the corresponding vibrational levels of the electronic states respectively.

The calculated values of N_v are to be regarded as relative values. The vibrational distribution in the CN bands after 500 ns of the laser pulse is given in Fig. 2. The inverse distribution observed for $v < 1$ in the case of the CN molecule is in accordance with the Franck–Condon principle. Similar inverse distributions are observed in certain other molecules also [45,46].

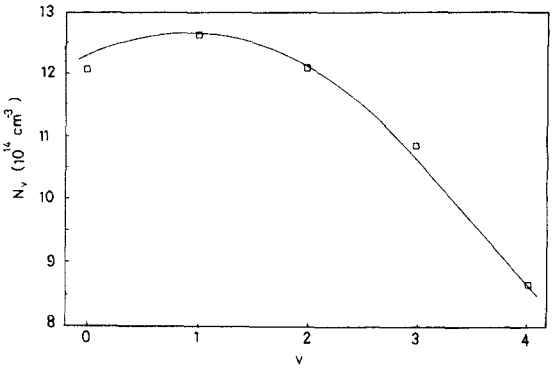

Fig. 2. The vibrational distribution of CN violet band (distance 10 mm, laser irradiance 3.54×10^{10} W cm^{-2}, delay 0.5 μs).

The LIP is usually taken to be in local thermodynamic equilibrium in order to evaluate plasma parameters such as number density, plasma temperature etc. In thermal equilibrium, the number densities at various vibrational levels of a molecule in the excited state can be evaluated using the Boltzmann distribution [44].

$$\ln \sum_{v''} (\lambda^4 I_{v'v''}) = C_1 - G(v')\left[\frac{hc}{kT_{\text{vib}}}\right] \tag{8}$$

where λ is the wavelength corresponding to each transition (v', v'') and $G(v')$ is the vibrational term value corresponding to the upper electronic state, C_1 is a constant, T_{vib} is the molecular vibrational temperature, h, the Plank's constant, k the Boltzmann constant and c, the speed of light. With measured intensities $I_{v'v''}$ and $G(v')$ we can plot a straight line as described by Eq. (8). The vibrational temperature is obtained from the slope of the Boltzmann plot between $\ln \Sigma_{v''} (\lambda^4 I_{v'v''})$ and $G(v')$. Typical Boltzmann plots of the band intensities against vibrational energy are given in Fig. 3. The advantage of using the Boltzmann distribution is that the information regarding the transition probability is not essential in this case.

3.3.1. Spatial dependence

One of the results in the present series of studies is that the spectral features are distinctly different for the emission from different sections of the plasma plume.

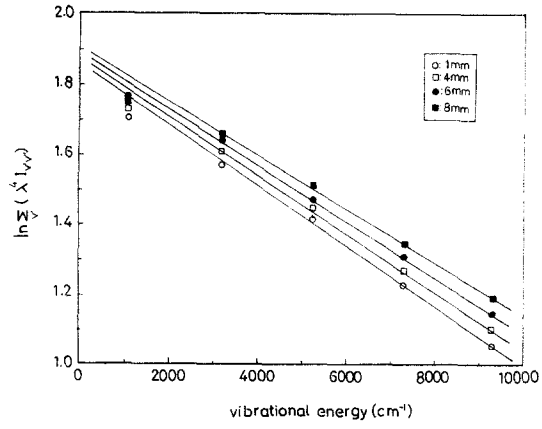

Fig. 3. Typical Boltzmann plots of vibrational band intensity vs vibrational energy for different distances from the target.

For spatial studies, different parts of the plasma were imaged onto the slit of the monochromator. Fig. 4 gives the typical CN violet band for different distances along the plasma expansion direction at a laser power density of 3.54×10^{10} W cm^{-2} and at a pressure 0.05 mbar. The continuum emission intensity in the plasma emission is greatest in the region close to the target surface and decreases sharply within a few millimeters from the target surface. The spectral emission intensity is very bright during the initial

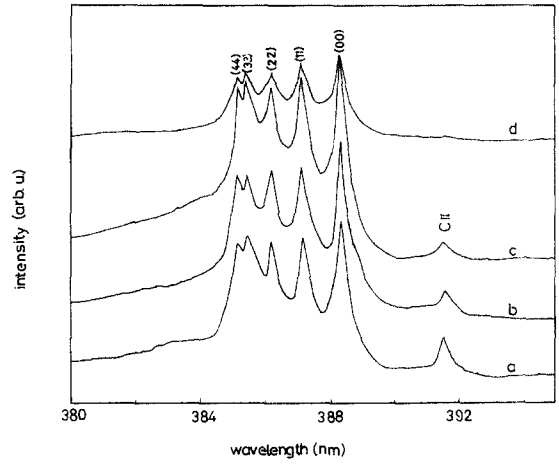

Fig. 4. CN violet band for $\Delta v = 0$ sequence at different spatial distances from the target (laser irradiance 3.54×10^{10} W cm^{-2} time delay 5 μs, (a) 2 mm, (b) 6 mm, (c) 10 mm, (d) 14 mm.

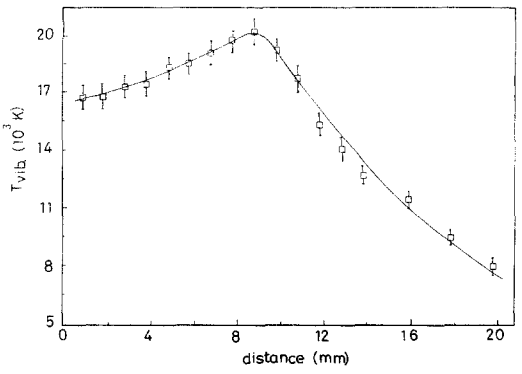

Fig. 5. The variation of vibrational temperature of the CN molecules with distance from the target for 5 μs delay time.

stages (up to 100 ns) of plume expansion due to Bremsstrahlung emission (free–free transition) from the hot plasma. In the region very close to the target surface, density in the plasma core is so high that much of the broadened line emission cannot be separated from the background. Farther away from the target surface, in the case of excited carbon species, the lines become narrower and weaker with increasing separation from the target.

The spatial variation of the vibrational temperature after a time interval of 5 μs with respect to the onset of ablation is given in Fig. 5. The average velocity being 6×10^5 cm s^{-1} [4], for an integration time of 100 ns, the spatial distance travelled by CN molecules is 0.6 mm, which is smaller than the successive spatial steps of 1 mm. In our present work the spatial resolution is better than 0.2 mm. Hence there will not be any significant mixing of spatial and temporal aspects of plasma.

It is found that at a particular laser irradiance, depending on the position of the sampled volume, the vibrational temperature of CN molecules varies. The spatial variation of vibrational temperature, 5 μs after the laser pulse, peaks at a distance 8 mm away from the target (20 000 K). The expected experimental error was ±10%. These results are also consistent with earlier reports on vibrational temperature of CN species [2,47,48].

The observed spatial variation of vibrational temperature can be explained as follows. Near the target surface the temperature is so high that collisional dissociation predominates and this causes a net decrease of the excitation of the higher vibrational levels with consequent reduction in band intensity. As we move away from the target, the collisional effects are reduced so that effectively the vibrational temperature is found to be high. At distances beyond an optimal value the decrease in plasma temperature will cause a reduction in vibrational temperature.

3.3.2. Time dependence

For the time dependence studies, emission spectra were recorded by varying delay times with respect to the laser pulse in the range 100–40 μs with the gate width of the boxcar averager fixed at 100 ns. All the spectra were recorded at a distance 7 mm away from the target. Fig. 6 gives the change in band head intensity of CN molecules ($\Delta v = 0$) at different time delays for a laser power density of 3.54×10^{10} W cm^{-2}. The emission characteristics of the plasma varied with time as illustrated in Fig. 6. Shortly after plasma initiation, the dominant radiation was a continuum mixed with ionic lines. The continuum emission is

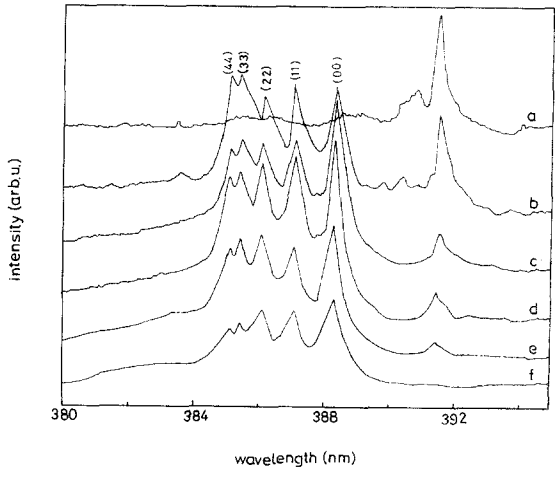

Fig. 6. CN violet band for $\Delta v = 0$ sequence at different time delays after the onset of plasma (laser irradiance 3.54×10^{10} W cm^{-2}, distance 7 mm) Time delays (a) 500 ns, (b) 1 μs, (c) 2 μs, (d) 4 μs (e) 10 μs and (f) 20 μs.

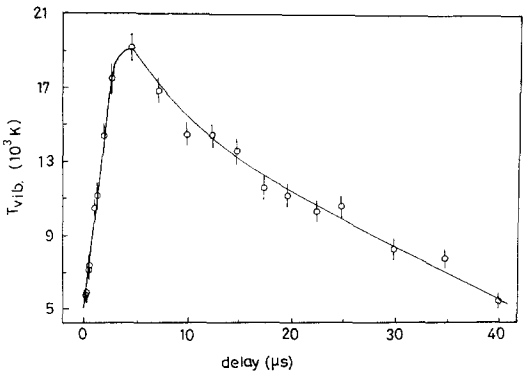

Fig. 7. Time dependence of vibrational temperature of CN molecule (laser irradiance 3.54×10^{10} W cm^{-2}, distance 7 mm).

due to Bremsstralung radiation and radiative recombination. Between 0.1 and 1 μs, both of these contributions decayed, leaving neutral lines and molecular bands which were seen up to 40 μs or longer. It has been observed that the individual emission lines from different atomic and ionic lines are highly Stark broadened during the initial stages of the plasma due to high plasma electron densities. At later times greater than 2 μs, the spectrum is dominated by CN violet system. It is to be noted that CN molecules are formed as a result of recombination of excited carbon species with ambient nitrogen present in the chamber as the hot plasma expands and cools. The time dependence of vibrational temperature is shown in Fig. 7. As it is clear from the figure there is a maximum vibrational temperature (19×10^3 K) after an elapse of 5 μs at a distance of 7 mm away from the target.

3.3.3. *Effect of laser irradiance*

The variation of vibrational temperature of CN molecules with laser energy at distances 5 and 10 mm from the target surface is given in Fig. 8. Such variation of vibrational temperature with laser power density occurs essentially due to the fact that comparatively large numbers of molecules are excited into higher vibrational levels with increasing laser irradiance. At 5 mm radial distance from the target surface, the vibrational temperature increases rapidly till laser power density reaches 6×10^{10} W cm^{-2} and after that it shows saturation behaviour. The saturation in vibrational temperature at higher irradiance may be due to following reasons. At higher laser irradiance the plasma temperature is so high that collisional dissociation/ionization predominates over recombination and causes a net decrease in the de-excitation rate of population in the higher vibrational levels and by plasma shielding which is due to the change in efficiency of laser coupling to the target by increased absorption and/or reflection by the plasma itself. At 10 mm radial distance from the target surface, a knee is found to occur in the curve showing variation of vibrational temperature at 4.2×10^{10} W cm^{-2}. This suggests the onset of possible nonlinear interactions such as self focusing of the laser beam within the plasma medium.

The self focusing phenomenon of laser beams in a plasma will occur if the Debye length (λ_D) is less than the laser beam diameter. The Debye length which is the characteristic screening length of the plasma is given by [49],

$$\lambda_D = \left[\frac{k_B T \epsilon_0}{N e^2}\right]^{1/2} \tag{9}$$

where k_B is the Boltzmann constant, T is the equilibrium plasma temperature, N is the equilibrium concentration, ϵ_0 is the permittivity and e

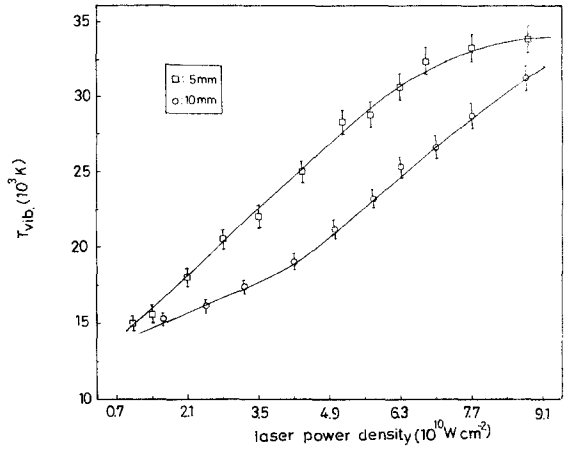

Fig. 8. The variation of vibrational temperature of the CN molecule with laser irradiance for different distances from the target.

is the electron charge. At 10 mm radial distance from the target surface, using the relative line intensity measurements of the successive ionization stages of the carbon species (as mentioned in Section 3.2.1), the estimated T_e and N_e are 19 700 K and 9.6×10^{16} cm^{-3}. Using these data, the Debye length is found to $\lambda_D = 0.03$ μm which is much less than the estimated beam diameter (200 μm). Such self focusing in the plasma leads to a higher effective power density resulting in an enhanced emission. Similar threshold like phenomenon is not perceptible at 5 mm radial distance from the target. Apparently this is due to the fact that a greater laser power density resulting from self focusing due to large plasma density and temperature lead to a much lower value for this threshold.

3.3.4. *Effect of ambient nitrogen*

The emission characteristics of the laser produced plasma are influenced to a large extend by the nature and composition of the surrounding atmosphere. A quantitative study of the effect of pressure on the relative intensities of the lines in the CN bands gives insight into the mechanism of formation of CN in its excited states and the mechanism of collisional energy transfer [50–52]. The change in vibrational temperature of CN molecules with respect to ambient nitrogen gas pressure inside the plasma chamber is given in Fig. 9 at a radial distance 3 mm away from the target and 3 μs after the irradiation at 3.5×10^{10} W cm^{-2}. The vibrational temperature peaks at 0.08 mbar and then falls quickly with increase in pressure and finally levels off at slightly lower value for T_{vib}. The highest rate of formation of excited CN molecules occurs at 0.08 mbar pressure under the above conditions. It can be noted that at higher nitrogen pressure the confinement of the plasma takes place. There can be competing nonradiative de-excitation processes which will be predominate at higher pressure of nitrogen gas in the chamber. Thus competition with collisional de-excitation results in reduced vibrational temperature as seen in Fig. 9.

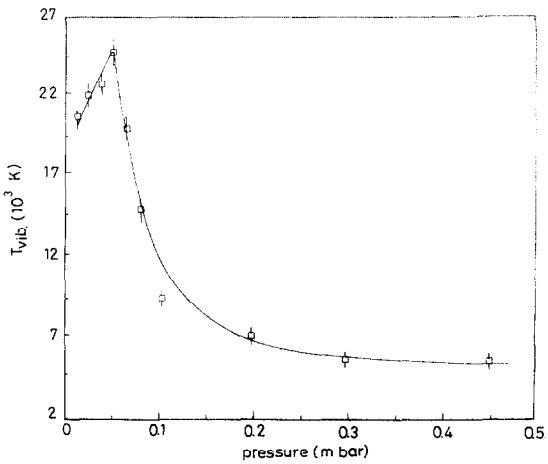

Fig. 9. The change in vibrational temperature for CN molecules with respect to ambient nitrogen gas pressure inside the plasma chamber (distance 3 mm, laser irradiance 3.54×10^{10} W cm^{-2}).

4. Conclusions

Extensive studies on the time and space resolved emission diagnostics have been carried out on the plasma produced by 1.06 μm radiation from a Q-switched Nd:YAG laser using graphite as the target. These investigations demonstrate that the emission intensities from CN species are sensitive to laser power density, pressure of the background gas, time after the elapse of laser pulse and spatial separation from the target. At low laser irradiance the emission bands due to C_2 and CN predominate while at higher irradiance the multiply ionized species up to C IV have been observed along with CN and C_2 species.

The vibrational temperature is found to increase with increase in laser power density and saturates at higher power levels. The saturation of vibrational temperature at higher power density is due to depletion of excited state population of CN molecules and by plasma shielding. The nonlinear interactions between the laser and the plasma give rise to the phenomenon of self focusing which exhibits threshold-like behaviour. The temperature and density of the plasma have been evaluated employing line intensity measurements and Stark broadening.

Acknowledgements

The present work is supported by the Department of Science and Technology, Government of India. One of the authors (SSH) is grateful to Council of Scientific and Industrial Research, New Delhi for a senior research fellowship. RCI, CVB and PG are thankful to University Grant Commission, New Delhi for their research fellowships.

References

[1] R.W. Dreyfus, R. Kelly, R.E. Walkup, Nucl. Instrum. Methods B 23 (1987) 557.
[2] G. Hatem, C. Colon, J.E. Campos, Spectrochim. Acta 49A (1993) 509.
[3] S.S. Harilal, R.C. Issac, C.V. Bindhu, V.P.N. Nampoori, C.P.G. Vallabhan, J. Appl. Phys. 80 (1996) 3561.
[4] S.S. Harilal, R.C. Issac, C.V. Bindhu, V.P.N. Nampoori, C.P.G. Vallabhan, Pramana J. Phys. 46 (1996) 145.
[5] Y. Iida, E.S. Yeung, Appl. Spectrosc. 48 (1994) 945.
[6] D.B. Chrisey and G.K. Hubler (Eds.), Pulsed Laser Deposition of Thin Films, John Wiley, New York, 1994.
[7] R.K. Singh, J. Narayanan, Phys. Rev. B 41 (1990) 8843.
[8] R.K. Singh, O.W. Holland, J. Narayanan, J. Appl. Phys. 68 (1990) 233.
[9] A. Krishnaswamy, J. Rangan, C. Narayanan, Appl. Phys. Lett. 54 (1989) 2455.
[10] S.S. Wagal, E.M. Juengerman, C.B. Collins, Appl. Phys. Lett. 53 (1988) 187.
[11] C.B. Collins, F. Davanloo, E.M. Juengerman, W.R. Osborn, D.R. Jander, Appl. Phys. Lett. 54 (1989) 216.
[12] F. Davanloo, E.M. Juengerman, D.R. Jander, T.J. Lee, C.B. Collins, J. Mater. Res. 5 (1990) 2398.
[13] G. Dollinger, P. Maier-Komor, Nucl. Instrum. Methods Phys. A 303 (1990) 50.
[14] R.K. Dwivedi, R.K. Thareja, Surf. Coat. Tech. 73 (1995) 170.
[15] A. Bykovskii Yu, A.G. Dudoladov, V.P. Kozlenkov, P.A. Leontev, JETP Lett. 20 (1994) 135.
[16] M. Ogmen, W.W. Duley, J. Phys. Chem. Solids 50 (1989) 1221.
[17] A.P. Malshe, S.M. Kanetlar, S.B. Ogale, ?.?. Krishsagar, J. Appl. Phys. 68 (1990) 5648.
[18] D.L. Pappas, K.L. Saenger, J.J. Cuomo, R.W. Dreyfus, J. Appl. Phys. 72 (1992) 3966.
[19] W. Kratschmer, L.D. Lamb, K. Fostiropoulos, D.R. Huffman, Nature 347 (1990) 354.
[20] P.S.R. Prasad, Abhilasha, R.K. Thareja, Phys. Stat. Sol. (a) 139 (1993) K1.
[21] S.S. Harilal, P. Radhakrishnan, V.P.N. Nampoori, C.P.G. Vallabhan, Appl. Phys. Lett. 64 (1994) 3377.
[22] R.C. William, J.T. Brenna, J. Chem. Phys. 92 (1990) 2269.
[23] V.P. Ageev, A.D. Akhasakhalyan, S.V. Gaponov, A.A. Gorbunov, V.I. Konov, V.I. Luchin, Sov. Phys. Tech. Phys. 33 (1988) 562.
[24] A.A. Voevodin, S.J.P. Laube, S.D. Walck, J.S. Solomon, M.S. Donley, J.S. Zabinski, J. Appl. Phys. 78 (1995) 4123.
[25] C. Boulmer-Leborgue, J. Hermann, B. Dubreuil, Plas. Sour. Sci. Tech. 2 (1993) 219.
[26] L.J. Radziemski and D.A. Cremers (Eds.), Laser induced plasmas and applications, Marcel Dekker Inc. New York, 1989.
[27] E.A. Rohlfing, J. Chem. Phys. 89 (1988) 6103.
[28] C.P. Safvan, F.A. Rajgara, V. Bhardwaj, G.R. Kumar, D. Mathur, Chem. Phys. Lett. 255 (1996) 25.
[29] S.S. Harilal, R.C. Issac, C.V. Bindhu, V.P.N. Nampoori, C.P.G. Vallabhan, Jpn. J. Appl. Phys. 36 (1997) 134.
[30] G. Padmaja, A.V. Ravi Kumar, V.P.N. Nampoori, C.P.G. Vallabhan, J. Phys. D. Appl. Phys. 26 (1993) 35.
[31] H.F. Sakeek, T. Morrow, W.G. Graham, D.G. Walmsley, Appl. Phys. Lett. 59 (1991) 3631.
[32] H.R. Griem, Spectral Line Broadening by Plasmas, Academic Press, New York, 1974.
[33] T. Okada, N. Shibamaru, Y. Nakayama, M. Maeda, Appl. Phys. Lett. 60 (1992) 941.
[34] D.B. Geohegan, in: J.C. Miller and R.F. Haglund (Eds.), Laser Ablation Mechanisms and Applications, Springer, Berlin, 1991.
[35] G.K. Varier, R.C. Issac, S.S. Harilal, C.V. Bindhu, V.P.N. Nampoori, C.P.G. Vallabhan, Spectrochim. Acta B (in press).
[36] Y. Tasaka, M. Tanaka, S. Usami, Jpn. J. Appl. Phys. 34 (1995) 1673.
[37] H. Kim, J.C. Postlewaite, T. Zyung, D. Dlott, Appl. Phys. Lett. 22 (1989) 2274.
[38] R. Engleman Jr, J. Mol. Spectrosc. 49 (1974) 106.
[39] C.V.V. Prasad, P.F. Bernath, C. Frum, R. Engleman Jr, J. Mol. Spectrosc. 159 (1992) 473.
[40] P.J. Knowles, H.J. Werner, P.J. Hay, D.C. Cartwright, J. Chem. Phys. 89 (1988) 7334.
[41] R.W.B. Pearse and A.G. Gaydon, The Identification of Molecular Spectra, Chapman and Hall, London, 1965.
[42] H.R. Griem, Plasma Spectroscopy, McGraw-Hill, New York, 1964.
[43] G. Bekfi, Principles of Laser Plasmas, Wiley, New York, 1974.
[44] G. Herzberg, Spectra of diatomic molecules, Molecular Spectra and Molecular Structure, 2nd edn., Van Nostrand, New York, 1950.
[45] M.A. MacDonald, S.J. David, R.D. Coombe, J. Chem. Phys. 84 (1986) 5513.
[46] J.R.L. Stephen, W.B. Charles, P.R. Alistair, J. Chem. Phys. 92 (1990) 300.
[47] X. Chen, J. Mazumder, A. Purohit, Appl. Phys. A 52 (1991) 328.

[48] J.A. Howe, J. Chem. Phys. 39 (1963) 362.
[49] T.P. Hughes, Plasmas and Laser Light, The institute of Physics, UK, 1975.
[50] N.H. Kiess, H.P. Broida, J. Mol. Spectrosc. 7 (1961) 194.
[51] A.T. Wager, Phys. Rev. 64 (1943) 18.
[52] H.T. Byck, Phys. Rev. 34 (1927) 453.